In situ measurement of the biogeochemical properties of Southern Ocean mesoscale eddies, in the Southwest Indian Ocean, April 2014

S. de Villiers[1], K. Siswana[1] and K. Vena[1]

[1]{Oceans and Coastal Research, Department of Environmental Affairs, Cape Town, South Africa}

Correspondence to: S. de Villiers (sdevilliers@gmail.com)

Abstract

Several open-ocean mesoscale features, a "young" warm-core (anti-cyclonic) eddy at 52°S, an "older" warm-core eddy at 57.5°S, as well as an adjacent cold-core (cyclonic) eddy at 56°S, were surveyed during a R/V S.A. Agulhas II cruise in April 2014. The main aim of the survey was to obtain hydrographical and biogeochemical profile data for contrasting open-ocean eddies in the Southern Ocean, that will be suitable for comparitive study and modelling of their heat, salt and nutrient characteristics, and the changes that occur in these properties as warm-core eddies migrate from the polar front southwards ~~into the Southern Ocean~~. The major result is that the older warm-core eddy at 57.5°S is, at its core, 2.7°C colder than a younger eddy at 52°S, while its dissolved silicate levels are almost 500% higher and accompanied by chlorophyll a levels that are more than 200% higher than that in the younger eddy. A total of 18 CTD stations were occupied in a sector south of the Southwest Indian Ridge, along three transects crossing several mesoscale features identified from satellite altimetry data prior to the cruise. The CTD data, as well as chlorophyll a and dissolved nutrient data (for NO_3^-, NO_2^-, PO_4^{3-} and SiO_2) have been processed, quality-controlled and made available via the PANGAEA Data Archiving and Publication database at http://doi.pangaea.de/10.1594/PANGAEA.848875.

Comment [S1]: Deleted in response to R#3

1 Introduction

The circulation and thermohaline structure of the Southern Ocean is of critical importance to global exchanges of heat, freshwater and biogeochemical constituents such as nutrients and CO_2. An detailed understanding of the role of mesoscale eddy transport in these processes is still lacking. It has only fairly recently been established that mesoscale eddies contain most of the kinetic energy of ocean circulation (Fu et al., 2010; Ferrari and Wunsch, 2009) and that the global zonal eddy volume transport is comparable in magnitude to that of the large-scale wind- and thermohaline-driven circulation (Zhang et al., 2014). It is estimated that in the open ocean most of the vertical transport of biogeochemical properties, such as nutrients, takes place at the sub-mesoscale, associated with eddies (Klein and Lapeyre, 2009; McGillicuddy et al., 2007; Lévy et al., 2001). At the global scale, areas of enhanced eddy kinetic energy usually also exhibit elevated levels of marine primary productivity (Chelton et al., 2011; Falkowski et al., 1991; Siegel et al., 2011). However, our understanding of the global significance of coincident large-scale patterns of enhanced open ocean productivity and mesoscale activity, and the importance of eddy-induced nutrient transport, is still in its infancy.

Progress in this field, including the incorporation of biogeochemical cycles into eddy-resolving GCM's, is severely limited by scarce *in situ* data, collected with the specific aim of improving our understanding of the physical and biogeochemical processes associated with mesoscale features such as eddies (Joyce et al., 1981; Mahadevan and Archer, 2010; Ansorge et al., 2010; Lehahn et al., 2011; Stramma et al., 2013; Chen et al., 2015). This scarcity of *in situ* data is particularly pronounced in the Southern Ocean. Despite the significance of the Southern Ocean to ocean-atmosphere CO_2 exchange and global climate, and the important role of ocean eddies to these processes (Frenger et al., 2013; Sheen et al., 2014; Morrow et al., 1994), it remains a remote, hostile and under-sampled ocean environment.

The objective of this paper is to present an overview of *in situ* data that had been collected in the Southern Hemisphere autumn, across a number of distinct mesoscale features in the southwestern Indian sector of the Southern Ocean (Fig. 1), and to make this data set available to the scientific community. Interaction of the Antarctic Circumpolar Current with the shallow topographic features of the Southwest Indian Ocean Ridge (SWIR) play an important role in the generation of open ocean eddies just south of the polar front (Gouretski and Danilov, 1994; Pollard and Read, 2001; Durgadoo et al., 2011; Ansorge et al., 2015).

Comment [S2]: Added in response to comment by R#2

Comment [S3]: "Ocean" deleted in response to R#3

Comment [S4]: Reference added as suggested

The subsequent movement of these eddies in a southerly direction, into the Southern Ocean proper, represents an ideal natural laboratory for the *in situ* observation and study of the eddy transport of heat, salt and chemicals across strong frontal zones in the Southern Ocean. To date, detailed studies of the chemical characteristics of such eddies and the evolution of these properties over time and distance, have not been carried out. This represents an important knowledge gap, particularly with regards to understanding Southern Ocean nutrient transport processes and carbon cycling.

2 Sampling survey design

The survey cruise was conducted from 02 April 2014 to 06 May 2014 (EXPOCODE 91AH20140402), the austral autumn, as part of the Department of Environmental Affairs' 2014 Marion Relief Voyage 011 on the MV SA Agulhas II, to its base in the subantarctic Prince Edward Islands (Fig. 1A). The MV SA Agulhas II is a relatively new (commissioned in 2012) polar research and supply vessel and is equipped with a moon pool, that can be used as a CTD launch area, even in the event of severe weather conditions.

Several months prior to the ship survey, evaluation of satellite altimetry sea surface height anomaly (SSHA) data was initiated, to identify and track the position of eddies suitable for study (Fig. 2). Composite SSHA satellite altimetry data, representing the sampling period, were obtained from the online data viewer of the Colorado Center for Astrodynamics Research (CCAR) (http://eddy.colorado.edu/ccar/data_ viewer/index) (Fig. 1B). The global Historical Gridded SSH data viewer was used, which is typically a composite of ± 10 days of Topex/Poseidon, Jason-a and Jason-2/OSTM data.

Mesoscale features with positive SSHA values, identified from satellite altimetry, were assumed to represent anti-cyclonic (counterclockwise rotation) eddies (Fig. 1B). Similarly, features with negative SSHA's ~~values~~ were assumed to be cyclonic (clockwise rotation) eddies. In the Southern Hemisphere, the centre or core of anti-cyclonic eddies are warm and sea surface height is elevated, whereas the core of cyclonic eddies are cold and characterised by negative SSHA's ~~values~~ (Chelton et al., 2013). Downwelling in the core of warm-core eddies and upwelling in the core of cold-core eddies have been inferred from isopycnal displacements (Zhang et al., 2014).

Observation of the evolution of the SSHA characteristics of mesoscale features over several months suggested that intense positive SSHA values can be assumed to represent younger, more recently formed, anti-cyclonic eddies (Fig. 2). Ship-based ADCP data (M. van

Comment [S5]: changed in response to R#1 and 3 comments

Comment [S6]: changed in response to reviewers comment

Comment [S7]: changed in response to R#3

Comment [S8]: changed in response to R#3

Comment [S9]: Text added in response to suggestion of R#3

Comment [S10]: Figure added in respone to reviewers' comments regarding the age and history of the eddies.

den Berg, unpublished cruise report contribution) confirmed the direction of ~~anti cyclonic and cyclonic~~ flow around these (Fig. 1B) mesoscale features.

On the basis of satellite SSHA images (Fig. 1B; Fig. 2), the following three main mesoscale features were identified for detailed study prior to the start of CTD transects, within the constraints of the ship-time available (based on approximate eddy core positions and SSHA at time of survey, Table 1):

- a "young, warm-core" anti-cyclonic eddy, at 52°S, 30.2°E (core SSHA > 40 cm)
- a "~~mature~~ older, warm-core" anti-cyclonic eddy, at 57.5°S, 29.5°E (core SSHA > 20 cm)
- a "cold-core" cyclonic eddy feature, at 56°S, 29.5°E (core SSHA < -20 cm)

The propagation path of each of the three these eddies were tracked using archived SSHA data (Fig. 2). The results show that about 6 months before the survey cruise, the "older" warm eddy occupied a similar latitude (about 52°S) than the "young" eddy sampled during the cruise. Also, the "cold-core" eddy had a similar southerly migration route and life history than the "older wamr-core" eddy. It is also interesting to note that 6 months after the survey, the "young" warm eddy ended up at approximately the same latitude that the "older" warm eddy was at, at the time of sampling (i.e. about 57.5°S).

Based on the identification of these three mesoscale features, the following three transects (E1 to E3 in Figure 1B) were ~~decided on~~ chosen for detailed CTD profiling (station locations in Table 1) and water column sampling for chemical analysis:

Transect E1 (15 to 16 April 2014): North-to-South transect from 55°S to 58.5°S, along 29.5°E; 8 CTD stations were occupied at 0.5° latitude intervals; the main features along this transect were the "mature" warm-core eddy and a cold-core cyclonic eddy just north of it;

Transect E2 (17 to 19 April 2014): East-to-West transect from 32°E to 28.25°E, along 57.5°S; 6 CTD stations were occupied along this transect, at 0.75° longitude intervals; the main feature along this transect is the mature warm-core eddy;

Transect E3 (21 to 22 April 2014): West-to-East transect along 52°S, from 28.3°E to 31°E; 4 CTD stations were occupied along this transect, at approximately 0.75° longitude intervals; the main feature along this transect was the relatively young, warm-core eddy.

Comment [S11]: deleted in response to R#3

Comment [S12]: Change made in response to reviewers' comment.

Comment [S13]: Added in response to reviewers' comments, and to provide context to the new Fig. 2

Comment [S14]: changed in response to R#3

Along all three transects the spacing of the stations (0.5° latitude and 0.75° longitude intervals) was constraint by the available ship time and weather conditions; although higher resolution spacing would have been more ideal, the spacing is sufficient to resolve the general structure of the eddies.

Comment [S15]: Text added in response to reviewer comments

3 Seawater sampling and analysis

Two SBE 9plus CTD systems, a moon pool CTD with a 24 20-L Niskin bottle rosette, or alternatively a 12 10-L Niskin bottle rosette for over-the-side deployment, were used for water column profiling and discrete water sampling at standard depths (20, 30, 40, 50, 75, 100, 150, 200, 300, 400, 500, 600, 700, 800, 900, 1 000, 1 250, 1 500, 2 000, 2 500, 3 000, 4 000, 5 000 m). The CTD deployments along the most southerly transects (E1 and E2), was conducted with the moon pool CTD. The moon pool CTD provides more and higher volume samples, but does not sample the upper 20 m of the water column. Unless sampling the upper 20 m is essential, the moon pool CTD alone is sufficient and preferable, and in extremely rough seas often the only option. If time and conditions allow, both CTD's can be deployed, in sequence, to maximize sampling resolution. The moon pool CTD was lost after completion of transects E1 and E2, as a result of damage sustained in very rough seas, and transect E3 was carried out with the smaller CTD only. The CTD temperature sensors were calibrated before and after the cruise, to ensure accuracy and achievement of the manufacturer's stated measurement precision of ±0.0001ºC. Salinity was computed from CTD data in practical salinity units (PSU) and the conductivity sensor calibrated using a combination of international standards and discrete samples, for every CTD cast, with the salinometer's stated measurement precision ±0.0001 PSU. The CTD oxygen sensor was calibrated with oxygen measurements obtained from discrete samples at selected depths for each CTD cast, applying the Winkler titration method using an electronic stand (Hansen, 1999). The precision of the oxygen titration was ±0.45 µmol/kg. Turbidity, given in Nepholometric Turbidity Units (NTU), was measured with a sensor connected to the CTD system, using the original calibration provided by the manufacturer~~company~~.

Comment [S16]: Added in response to comment by R#! and #3

Comment [S17]: Text added for clarificaiton, in response to comments by R#2 and #3

Comment [S18]: Added for clarifation, as requested by all reviewers

Comment [S19]: Changed in response to R#3

Seawater samples for chemical analyses were collected from the Niskin bottles, at the standard depths detailed earlier. Samples for dissolved oxygen analysis were collected from the Niskin bottles via silicone tubing, taking care not to introduce or trap air bubbles. For dissolved inorganic nutrient analysis, acid-washed 15 mL polypropylene tubes were thoroughly rinsed with sample water before filling and frozen at -80 °C prior to ship-based

analysis using an Astoria AutoAnalyser Series 300, expanded to four channels. Dissolved nitrate (NO_3^-), nitrite (NO_2^-) and silicate (SiO_2) were determined following the methods of Armstrong et al. (1967) and phosphate (PO_4^{3-}) according to the methods of Bernhardt and Wilhelms (1967), with typical in run precision of ± 0.1 µmolL^{-1} for NO_3^- and NO_2^-, ± 0.02 µmolL^{-1} for PO_4^{3-} and ± 0.24 µmolL^{-1} for SiO_2.

Samples for chlorophyll a analysis were taken at four depths (near-surface, above the fluorescence maximum (F-max), F-max and below the F-max), with the depth of F-max established from the downcast, continuous CTD fluorescence profile. Seawater samples (200 ml) for chlorophyll a analysis were collected in pre-rinsed plastic bottles. Samples were immediately filtered, under vacuum onto 25 mm Whatman™ GF/F glass fibre filter papers (Parsons et al., 1984). The filter papers were frozen in aluminium foil pouches for storage until analysis~~prior to analysis~~. Chlorophyll a was measured fluorometrically on a Turner Designs 10-AU fluorometer after extraction in 90% acetone (Welschmeyer, 1995), with a precision of approximately 5%. The fluorometer was calibrated with chlorophyll a standard (Sigma Chemical Co., USA) in 90% acetone solution with a GBC Cintra 404 spectrophotometer and an extraction coefficient of 87.67 Lg^{-1}cm^{-1}.

4 Data overview and Discussion

In situ CTD profiling data (Fig. 3A-B-C and Fig. 4) confirmed the presence and position of the anti-cyclonic and cyclonic eddies, targeted for this study based on SSHA observational data (Fig. 1). The average values of physical and chemical parameters for the upper 100 m of the water column is summarized for all CTD stations in Table 2 and profile data for temperature, salinity, nutrients and chlorophyll a are shown in Fig. 3, ~~Fig.~~ 5 and ~~Fig.~~ 6. These data demonstrate a number of significant differences between the eddies, most notably:

- The old, warm (or anti-cyclonic) eddy at 57.5°S (Table 1) has a maximum core temperature of 2.2 to 2.35°C, which is observed in the 200 to 300 m depth range (Fig. 4). In the core of the cold-core eddy located 1.5° north of the core of the older warm-core feature, temperature reaches a value of almost 1.85°C in the upper 100 m of the water column. The young, warm-core eddy much further north at 52°S, in contrast, is characterised by core temperatures of around 4.7°C in the well-mixed upper 100 m layer, and around 3 to 2.6°C in the 200 to 300 m depth range. The sampling survey, therefore, successfully captured the

Comment [S20]: Added in response to reviewers' requests.

Comment [S21]: Added in response to comment by R#2

Comment [S22]: changed in response to comment by R#3

Comment [S23]: This section has been substantially rewritten and re-organized, in response to reviewers' comments.

Comment [S24]: corrected as suggested by R#3

Comment [S25]: corrections as suggested by R#3

Comment [S26]: amended as suggested by R#3

Comment [S27]: amended as suggested by R#3

Comment [S28]: changes made in response to suggestion by R#3

different temperature characteristics of ~~eddies with contrasting origins and histories~~ cyclonic and anti-cyclonic eddies at different stages in their maturity.

- In the upper 100 m, the young warm-core eddy ~~(E3 3)~~ is 2.74°C warmer, ~~slightly~~ less saline by 0.21 psu, with silicate levels ~ 80% lower and chlorophyll a levels more than a factor of 2 lower~~,~~ than that in its older warm-core quivalent further south ~~(E1 6)~~

- In contrast, t~~T~~he upper ocean water characteristics of the cold-core and older warm-core eddies, at 56°S and 57.5°S respectively, are much more similar to each other than is the case for the younger versus older warm-core eddies (Table 2). The cold eddy is, on average, only 0.13°C colder than the older warm-core eddy, with approximately the same upper ocean salinity values. The older warm-core eddy has slightly higher upper ocean phosphate and nitrate concentrations than the cold-core eddy, 6% and 5% respectively, but has significantly higher chlorophyll a l (+63%) and lower silicate levels (-17%).

The data show that the most notable differences between the young and older warm-core eddies are their surface ocean dissolved silicate and chlorophyll a characteristics. One possible explanation is that, as warm-core eddies migrate in a southerly direction (Fig. 2), lateral and/or vertical mixing with adjacent silicate-rich water masses results in increasing surface silicate levels. These higher silicate levels, together with potential additional controls such as light and iron availability, then results in dramatically increased levels of productivity. Bongo net tows conducted during the survey (unpublished results), confirmed that the increased levels of chlorophyll a, south of the polar front, are associated with diatom productivity. Alternatively, if it is more appropriate to think of eddies as local (but persistent) perturbations in the density structure, then higher silicate values in the older, warm-core eddy is simply consistent with the characteristics of water masses south of the polar front compared to further north.

In summary, the *in situ* nutrient and chlorophyll a profile data presented here provide valuable input data for the modelling of the complex biogeochemical processes associated with mesoscale activity in the Southern Ocean.

Comment [S29]: Changes as suggested by R#3

Comment [S30]: deleted in response to comment by R#3

Comment [S31]: changed in response to R33

Comment [S32]: changed as suggested by R#1

Comment [S33]: deleted comman in response to R#3

Comment [S34]: deleted in response to comment by R#3

Comment [S35]: changed in response to R#3 comment

Comment [S36]: added as suggested by R#3

Comment [S37]: changed as suggested by R#2

Author contributions

S. de Villiers determined the sampling strategy, collected samples, and oversaw and collated the measurements; K. Siswana and K. Vena assisted in sample collection, chemical analysis and data presentation; S. de Villiers prepared the manuscript.

Acknowledgements

All ship-based participants, crew and research staff, in some way or another contributed to the collection of this dataset, and their contributions are gratefully acknowledged. The Chief Scientist for the cruise was Dr. H. Verheye, and the cruise and associated research activities were financed by the Department of Environmental Affairs.

References

Ansorge, I.J., Jackson, J.M., Reid, K., Durgadoo, J.V., Swart, S., and Eberenz, S.: Evidence of a southward eddy corridor in the South-West Indian ocean, Deep-Sea Res. II, 119, 69-76, 2015.

Ansorge, I.J., Pakhomov, E.A., Kaehler, S., Lutjeharms, J.R.E., and Durgadoo, J.V.: Physical and biological coupling in eddies in the lee of the South-West Indian Ridge, Polar Biol., 33, 747-759, 2010.

Armstrong, F.A.J., Stearns, C.A., and Strickland, J.D.H.: The measurement of upwelling and subsequent biological processes by means of the Technicon Autoanalyzer and associated equipment, Deep-Sea Res., 14, 381-389, 1967.

Bernhardt, H., and Wilhelms, A.: The continuous determination of low level iron, soluble phosphate and total phosphate with the AutoAnalyzer, Technicon Symposia I, 385-389, 1967.

Chelton, D.: Mesoscale eddy effects, Nat. Geosci., 6, 594-594, 2013.

Chelton, D.B., Gaube, P., Schlax, M.G., Early, J.J., and Samelson, R.M.: The influence of nonlinear mesoscale eddies on near-surface oceanic chlorophyll, Science, 334, 328-332, 2011.

Chen, Y.L., Chen, H-Y., Jan, S., Lin, Y-H., Kuo, T-H., and Hung, J-J.: Biologically active warm-core anticyclonic eddies in the marginal seas of the western Pacific Ocean, Deep Sea Res. I, 106, 68-84, 2015.

Dong, S., Sprintall, J., and Gille, S.T.: Location of the Antarctic Polar Front from AMSR-E satellite sea surface temperature measurements, J. Phys. Ocean., 36, 2075-2089, 2006.

Durgadoo, J.V., Ansorge, I.J., de Cuevas, B.A., Lutjeharms, J.R.E., and Coward, A.C.: Decay of eddies at the South-West Indian Ridge, S. Afr. J. Sci., 107 (11/12), Art. #673, dx.doi.org/10.4102/sajs.v107i11/12.673, 2011.

Falkowski, P., Ziemann, D., Kolber, Z., and Bienfang, P.: Role of eddy pumping in enhancing primary production in the ocean, Nature, 352, 55-58, 1991.

Ferrari, R., and Wunch, C.: Ocean circulation kinetic energy: reservoirs, sources, and sinks, Ann. Rev. Fluid Mech., 41, 253-282, 2009.

Frenger, I., Gruber, N., Knutti, R., and Münnich, M.: Imprint of Southern Ocean eddies on winds, clouds and rainfall, Nat. Geosci., 6, 608-612, 2013.

Fu, L.-L., Chelton, D.B., Le, P.-Y., and Morrow, R.: Eddy dynamics from satellite altimetry, Oceanography, 23(4), 14-25, 2010.

Gouretski, V.V, and Danilov, A.I.: Characteristic of warm rings in the African sector of the Antarctic Circumpolar current, Deep-Sea Res., 41, 1131-1157, 1994.

Hansen, H.P.: Determination of oxygen, in: Methods of Seawater analysis, edited by: Grasshoff, K.K., and Ehrhardt M., Wiley-VCH, Weinheim, 75-89, 1999.

Joyce, T.M., Patterson, S.L., and Millard Jr., R.C.: Anatomy of a cyclonic ring in the Drake Passage, Deep-Sea Res., 28(11A), 1265-1287, 1981.

Klein, P., and Lapeyre, G.: The oceanic vertical pump induced by mesoscale and submesoscale turbulence, Ann. Rev. Mar. Sci., 1, 351-375, 2009.

Lehahn, Y., d'Ovidio, F., Lévy, M., Amitai, Y., and Heifetz, E.: Long range transport of a quasi isolated chlorophyll patch by an Agulhas ring, Geophys. Res. Lett., 38, L16610, doi:10.1029/2011GL048588, 2011.

Lévy, M., Klein, P., and Treguier, A.-M.: Impact of sub-mesoscale physics on production and subduction of phytoplankton in an oligotrophic regime, J. Mar. Res., 59, 535-565, 2001.

Mahadevan, A., and Archer, D.: Modeling the impact of fronts and mesoscale circulation on the nutrient supply and biogeochemistry of the upper ocean, J. Geophys. Res., 105, 1209-1225, 2000.

McGillicuddy, Jr., D.J., Anderson, L.A., Bates, N.R., et al.: Eddy/wind interactions stimulate extraordinary mid-ocean plankton blooms, Science, 316, 1021-1026, 2007.

Morrow, R.A., Coleman, R., Church, J.A., and Chelton, D.B.: Surface eddy momentum flux and velocity variance in the Southern Ocean from GEOSAT altimetry, J. Phys. Ocean., 24, 2050-2071, 1994.

Parsons, T.R., Maita, Y., and Lalli., C.M.: A Manual of Chemical and Biological Methods for Seawater Analysis, Pergamon Press, Oxford, 173 pp., 1984.

Pollard RT, Read JF. Circulation pathways and transports of the Southern Ocean in the vicinity of the Southwest Indian Ridge. J Geophys Res. 2001;106:2881–2898. http://dx.doi.org/10.1029/2000JC900090.

Sheen, K.L., Garabato, A.C.N., Brearley, J.A., et al.: Eddy-induced variability in Southern Ocean abyssal mixing on climatic timescales, Nat. Geosci., 7, 577-582, 2014.

Siegel, D., Peterson, P., McGillicuddy, D., Maritorena, S., and Nelson, N.: Bio-optical footprints created by mesoscale eddies in the Sargasso Sea, Geophys. Res. Lett., 38(13), L13608, 2011.

Stramma, L., Bange, H.W., Czeschel, R., Lorenzo, A., and Frank, M.: On the role of mesoscale eddies for the biological productivity and biogeochemistry in the eastern tropical Pacific Ocean off Peru, Biogeosci., 10, 7293-7306, 2013.

Welschmeyer, N.A., and Waterhouse, T.Y.: Taxon-specific analysis of microzooplankton grazing rates and phytoplankton growth rates, Limnol. Oceanogr., 40(4), 827-834, 1995.

Zhang, Z., Wang, W., and Qui, B.: Oceanic mass transport by mesoscale eddies, Science, 345, 322-324, 2014.

Table 1. CTD station locations and identification of CTD station positions relative to eddy cores, as inferred from altimetry data. E1, E2 and E3 refer to the three transect lines shown in Figure 1. Based on interpretation of relative SSH anomalies, E1-6 is the core of the older warm-core eddy, E1-3 that of a cold-core eddy, and E3-3 that of the young warm-core eddy.

Comment [S38]: added as suggested by R#2 and #3

Ship Station	ID	Position relative to eddy core	Sampling Date	Latitude (°S)	Longitude (°E)	Depth (m)
AM00264	**E1-1**	1°N of cold-core	15 April 2014	55.0	29.5	4506
AM00265	**E1-2**	0.5°N of cold-core	15 April 2014	55.5	29.5	5296
AM00266	**E1-3**	Cold-core	15 April 2014	56.0	29.5	5581
AM00267	**E1-4**	0.5°S of cold-core	15 April 2014	56.5	29.5	5288
AM00268	**E1-5**	0.5°N of warm-core	16 April 2014	57.0	29.5	5275
AM00269	**E1-6**	Warm-core	16 April 2014	57.5	29.5	5565
AM00270	**E1-7**	0.5°S of warm-core	16 April 2014	58.0	29.5	5261
AM00271	**E1-8**	1°S of warm-core	16 April 2014	58.5	29.5	5534
AM00272	**E2-1**	2.5°E of warm-core	17 April 2014	57.5	32.0	5550
AM00273	**E2-2**	1.75°E of warm-core	18 April 2014	57.5	31.3	5262
AM00274	**E2-3**	1°E of warm-core	18 April 2014	57.5	30.5	5270
AM00275	**E2-4**	0.25°E of warm-core	18 April 2014	57.5	29.8	5269
AM00276	**E2-5**	0.5°W of warm-core	19 April 2014	57.5	29.0	5268
AM00277	**E2-6**	1.25°W of warm-core	19 April 2014	57.5	28.3	5135
AM00281	**E3-1**	1.9°W of warm-core	21 April 2014	52.0	28.3	5481
AM00282	**E3-2**	0.73°W of warm-core	22 April 2014	52.0	29.5	5379
AM00283	**E3-3**	Warm-core	22 April 2014	52.0	30.2	3817
AM00284	**E3-4**	0.78°E of warm-core	22 April 2014	52.0	31.0	5154

Comment [S39]: number of deciman places reduced as suggested by R#2

Table 2. Average upper ocean (surface to 100 m depth) physical and chemical water column characteristics, obtained from CTD profiles, in and around warm and cold eddies. Samples for nutrient and chlorophyll a analysis were not collected at CTD stations E2-1 and E3-1.

ID	**Position relative to eddy core**	**T** (^{o}C)	**S** (PSU)	**SiO_2** (µmol/kg)	**PO_4^{3-}** (µmol/kg)	**NO_3^-** (µmol/kg)	**Chl-a** (µg/L)
E1-1	1^{o}N of cold-core	2.31	33.97	29.9	1.50	20.9	0.14
E1-2	0.5^{o}N of cold-core	1.75	33.98	29.6	1.37	20.4	0.33
E1-3	Cold-core	1.83	33.98	30.8	1.47	21.6	0.35
E1-4	0.5^{o}S of cold-core	1.99	33.95	29.3	1.58	23.6	0.36
E1-5	0.5^{o}N of warm-core	1.77	33.96	27.6	1.53	22.7	0.58
E1-6	Warm-core	1.96	33.98	25.7	1.56	22.7	0.57
E1-7	0.5^{o}S of warm-core	0.88	33.87	34.8	1.56	23.3	0.31
E1-8	1^{o}S of warm-core	1.04	33.93	35.2	1.51	22.3	0.23
E2-1	2.5^{o}E of warm-core	1.09	33.92				
E2-2	1.75^{o}E of warm-core	1.27	33.99	31.2	1.46	20.1	0.44
E2-3	1^{o}E of warm-core	1.71	33.96	26.2	1.51	21.5	0.49
E2-4	0.25^{o}E of warm-core	1.62	33.97	29.0	1.56	22.5	0.33
E2-5	0.5^{o}W of warm-core	1.60	33.96	29.7	1.60	22.7	0.44
E2-6	1.25^{o}W of warm-core	1.60	33.98	29.1	1.49	22.4	0.42
E3-1	1.9^{o}W of warm-core	1.69	34.04				
E3-2	0.73^{o}W of warm-core	3.45	33.80	13.7	1.39	21.9	0.24
E3-3	Warm-core	4.70	33.77	4.4	1.34	20.2	0.18
E3-4	0.78^{o}E of warm-core	4.76	33.77	3.5	1.34	19.5	0.18

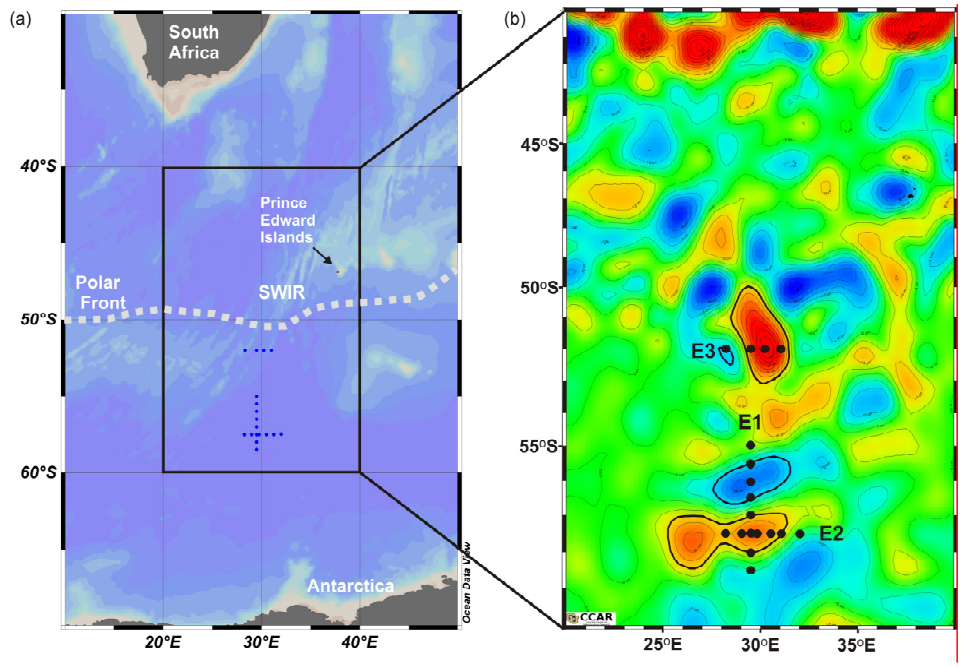

Figure 1. **A**: Seafloor bathymetry in the southwestern Indian Ocean sector of the Southern Ocean, to indicate the position of the Southwest Indian Ridge (SWIR); shown in grey is the average position of the Polar Front (adapted from Dong et al., 2006); **B**: The CTD station locations along transect lines E1 to E3 are shown in black dots superimposed upon a satellite altimetry map; red indicates positive SSHA's and blue indicates negative SSHA's.~~Superimposed upon a satellite altimetry map is the position of the transect lines, E1 to E3, situated between 52°S to 58.5°S, south of the Prince Edward Island group; black dots indicate the location of CTD stations; red positive SSHA values and blue negative SSHA values~~. SSHA contour intervals are 5 cm, and the -10 cm and +10 cm contour lines that the transect lines cross, are highlighted with solid black lines.

Comment [S40]: degree S symbols added to B (suggested by R#3); 10 cm SSHA contours now highlighted as suggested by R#1 and #3

Comment [S41]: changes recommended by R#3

Comment [S42]: Text added in response to comment #1 and #2

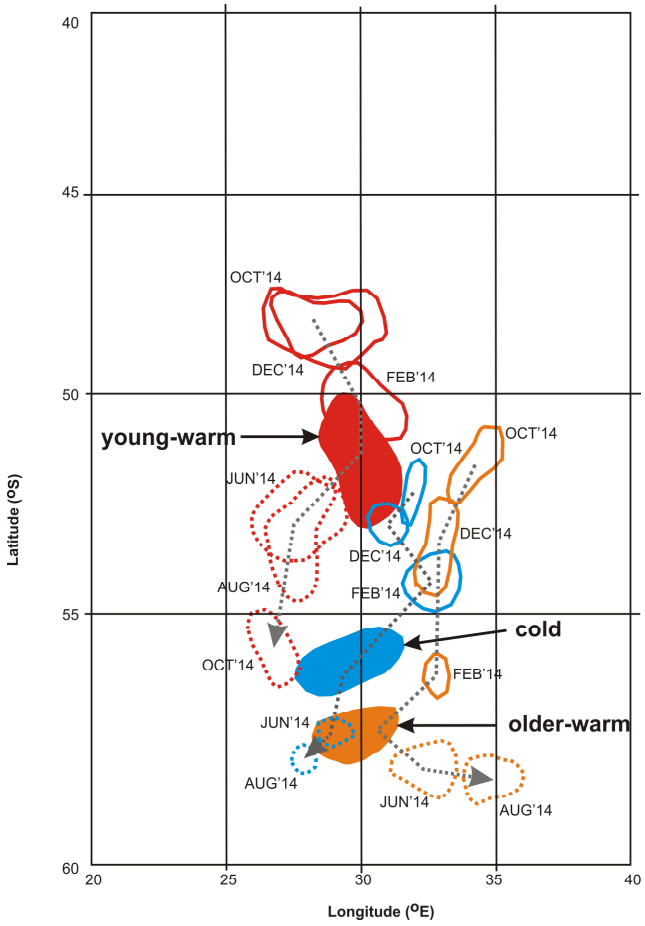

Figure 2. Eddy migration tracks, as inferred from SSHA archive data. Solid red, blue and orange areas, respectively, reflect the area inside the 10 cm SSHA contour for the young, warm-core, cold-core and older, warm-core eddies, at the time of sampling. Solid red, blue and orange lines, similarly, indicate the position of the eddies (and the extent of the eddy within the 10 cm SSHA contour) prior to sampling, at 2 monthly intervals, as indicated by the labels. Broken red, blue and orange lines indicate the position of the eddies subsequent to sampling, again at 2 monthly intervals. Black arrows are used to highlight the southerly migration of the eddies.

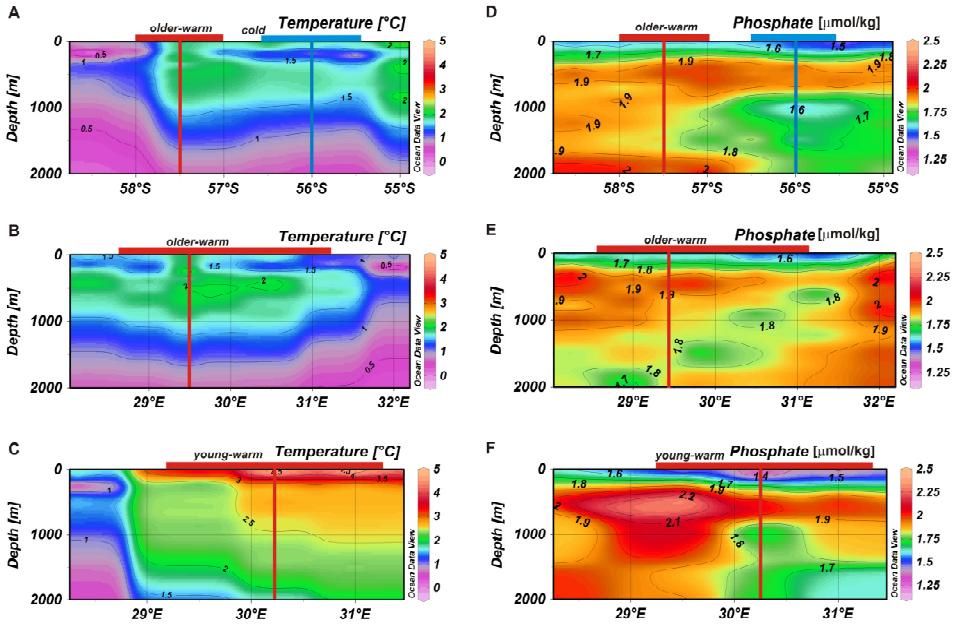

Figure 3. Temperature and dissolved phosphate profile data to a depth of 3,000 m, for Transect E1 (**A** and **D**), Transect E2 (**B** and **E**) and Transect E3 (**C** and **F**). Vertical red lines (at 57.5°S in A and D, 29.5°E in B and E, and 30.25°E in C and F), indicate the approximate position of the center of the older and young warm-core eddies, respectively, and vertical blue lines (at 56°S in A and D) similarly indicate the position of the cold-core eddy. The horizontal red and blue bars above these vertical red lines, in turn, indicate the estimated horizontal extent of the eddies, within the 10 cm SSHA contour intervals.

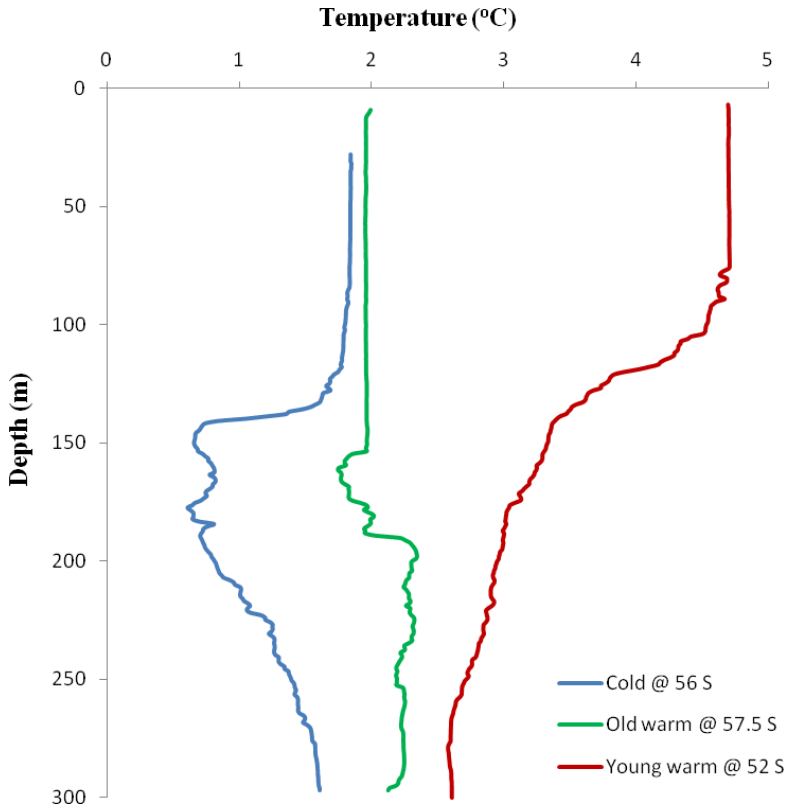

Figure 4. Upper 300 m water column temperature profiles, from CTD stations located at the approximate cores of the three main mesoscale features present along the transect lines: in blue the cold-core eddy (CTD station E1-3 in Table 1), in green the older warm-core eddy (E1-6) and in red the young warm-core eddy (E3-3).

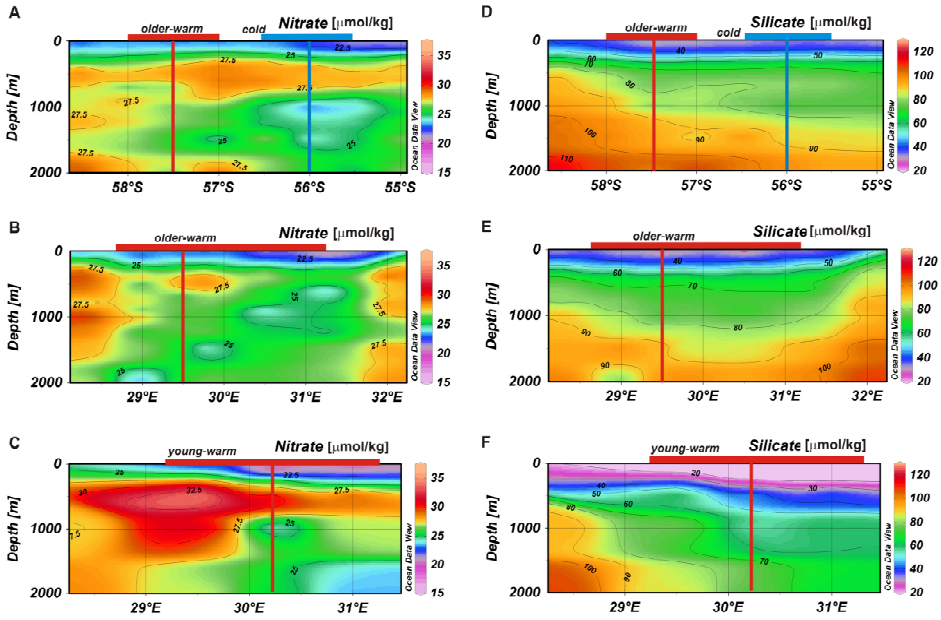

Figure 5. Dissolved nitrate and silicate profiles, plotted to a depth of 3,000 m, for Transect E1 (**A** and **D**), Transect E2 (**B** and **E**), and Transect E3 (**C** and **F**). Vertical red and blue lines represent the eddy cores as described for Fig. 3. The data available online can be used to reproduce these Ocean Dataviewer plots, to shallower or deeper depths.

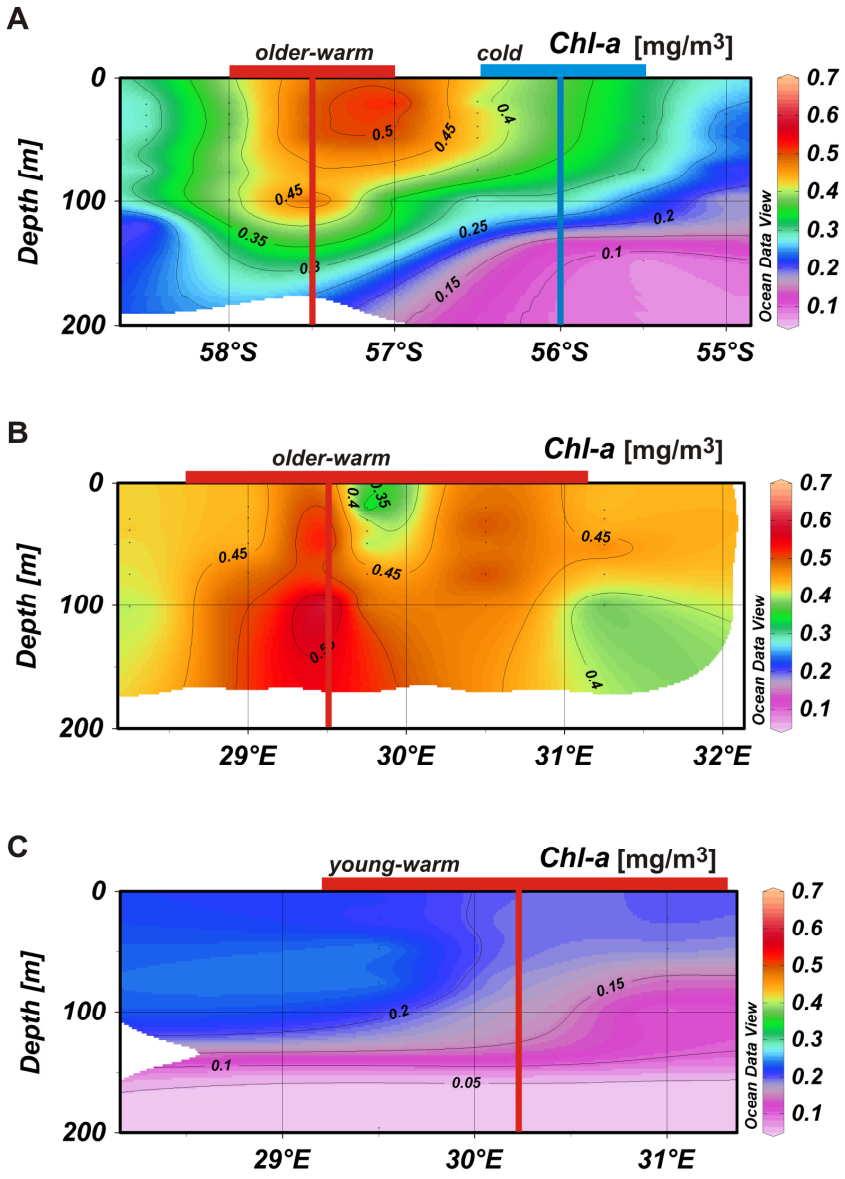

Figure 6. Chlorophyll a profiles, plotted to a depth of 200 m, for Transect E1 (**A** and **D**), Transect E2 (**B** and **E**), and Transect E3 (**C** and **F**). Vertical red and blue lines represent the eddy cores as described for Fig. 3. The data available online can be used to reproduce these Ocean Dataviewer plots, to shallower or deeper depths.